TR3 enhances AR Variant Production and Transactivation, Increasing Androgen Independency of AR Signaling in Prostate Cancer Cells

Tuyen Thanh Tran
Chonnam National University
Keesook Lee (klee@chonnam.ac.kr)
Chonnam National University https://orcid.org/0000-0002-0074-4355

Research

Keywords: TR3, androgen receptor, AR splicing variants, androgen-independent activity, castration-resistant prostate cancer.

Posted Date: May 7th, 2021

DOI: https://doi.org/10.21203/rs.3.rs-432174/v1

Abstract

Background

Increased expression of constitutively active androgen receptor variants (AR-Vs) is associated with the development of advanced castration-resistant prostate cancer. The pro-oncogenic function of TR3, an orphan nuclear receptor, has been reported in various cancers including prostate cancer. However, the roles of TR3 in androgen receptor (AR) expression and signaling in prostate cancer cells are poorly understood.

Methods

Western blotting and quantitative RT-PCR were used to evaluate AR and AR-V expression levels affected by TR3 expression level. RNA-seq analysis, coimmunoprecipitation, cross-linked RNA-immunoprecipitation, and single-strand RNA protection and pull-down assays were conducted to elucidate the molecular mechanisms by which TR3 affected AR-V production.

Results

Database analysis revealed that TR3 expression level is elevated in prostate tumors, and is positively correlated with that of AR. TR3 overexpression increased the production of AR splice variants in addition to general upregulation of AR expression. TR3 interacted with some spliceosomal complex components and AR precursor mRNA, altering the splice junction rates between exons. TR3 also enhanced androgen-independent AR function. Furthermore, TR3 overexpression increased cell proliferation and mobility of AR-positive prostate cancer cells and stimulated tumorigenesis of androgen-independent prostate cancer cells in mouse xenograft models. This is the first study to report that TR3 is a multifunctional regulator of AR signaling in prostate cancer cells.

Conclusions

TR3 alters AR expression, splicing process, and activity in prostate cancer cells, increasing the androgen independency of AR signaling. Therefore, TR3 may play a crucial role in the progression of prostate cancer to advanced castration-resistant form.

Background

Prostate cancer is one of the leading lethal malignancies in males, and androgen receptor (AR), a ligand-dependent transcription factor, plays a pivotal role in the development, progression, and metastasis of prostate cancers [1]. AR has three main functional domains: NH2-terminal transactivation domain (NTD), DNA-binding domain, and ligand-binding domain (LBD). Increased expression of constitutively active AR

variants (AR-Vs), which lack LBD, is associated with the development of advanced castration-resistant prostate cancer (CRPC), leading to the failure of hormone therapy [2]. Among the multiple AR-Vs reported, AR-V7 (AR3) is the most common in prostate cancer cell lines and tumors and is generated by splicing between exon 3 and cryptic exon 3 (CE3) as well as exon 3 duplication [3]. Mutations and genomic rearrangements are the two major causes of multiple drug resistance during prostate cancer progression, especially during the development of advanced CRPCs [4, 5]. These mutations and genomic rearrangements result in the generation of alternative promoters and cryptic splice sites that drive an alternative splicing process.

Several splicing factors have been found to be associated with alternative splicing events in the AR precursor mRNA (pre-mRNA) in prostate cancer cells. Among these, heterogeneous nuclear ribonucleoprotein (hnRNP) A2B1, hnRNP E1/E2, and HUR (ELAV-like protein 1, ELAVL1) are RNA-binding proteins (RBPs) that bind to AR pre-mRNA and regulate the expression of AR-Vs in advanced CRPCs [6, 7]. hnRNP E1/E2 contains KH domains and HUR contains RRM domains, and both of these domain types bind to the UC-rich region in AR pre-mRNA [6]. In contrast, hnRNP A/B proteins, especially hnRNP A1 and A2B1, which contain RRM domains, bind to AR pre-mRNA splice sites, and enhance the expression of some AR-Vs, particularly AR-V7, AR-V1, AR-V4, and AR-V5, in CRPCs [7]. Enrichment of hnRNP A1/A2B1 at splice sites involved in AR-V production was further increased in enzalutamide-resistant prostate cancer cells [7]. Additionally, NOVA-2 is an alternative splicing factor, whose expression is upregulated in some cancers [8], although its role in prostate cancer is poorly understood. It is a KH domain-containing RBP, which binds to the YCAY sequence in RNA and regulates the stabilization and transport of intron-excised RNA.

Human orphan nuclear receptor TR3 (also known as NR4A1) is an immediate early response gene induced by a diverse range of signals, including stressors, cytokines, growth factors, and small molecular compounds. TR3 expression is associated with many physiological and pathological processes, such as cell survival and death, inflammation, and cancer development [9]. TR3 is upregulated in many cancers, including lung, colorectal, breast, and prostate cancers [10]. In addition, TR3 signaling activation enhances cancer cell proliferation and tumor progression [10], while loss of TR3 function by retinoid and its derivative compounds induces apoptosis [11]. TR3 overexpression increases prostate cancer cell viability [10]. However, the roles of TR3, especially in AR expression and signaling, are poorly understood.

The present study is the first to demonstrate that TR3 affects AR splicing process as well as its expression and further enhances androgen-independent AR activity in prostate cancer cells. These results, together with the stimulation of tumorigenesis by TR3 overexpression, suggest that TR3 is a pivotal controller of AR signaling in prostate cancer cells and plays a crucial role in cancer progression and the maintenance of advanced CRPCs.

Materials And Methods

Cell lines

LNCaP (CRL-1740) and HEK 293T (CRL-11268) cells were purchased from the American Type Culture Collection (ATCC, Manassa, VA, USA). The C4-2, CWR22rv, and PC3 cell lines were kindly provided by Dr. C Jung (Chonnam National University Medical School). PPC1 and DU145 cells were received from Dr. S Baek (Seoul National University, Republic of Korea). A recombinant adenovirus E1 expressing HEK-293 (Ad293) cells were purchased from Agilent Technologies, Inc. (Santa Clara, CA 95051, USA). LNCaP, C4-2, CWR22rv, and PC3 cells were maintained in RMPI-1640 media (HyClone, USA) with 5% fetal bovine serum (FBS) (Gibco, USA). PPC1 and HEK 293T cells were cultured in DMEM (HyClone, USA) with 10% FBS. Media containing 5% charcoal-stripped serum (cFBS) was used for the starvation and steroid studies. All cell lines were maintained in the presence of 100 units/ml penicillin and 100 mg/ml streptomycin (Gibco, USA) in a 5% CO_2 incubator at 37°C.

Generation of inducible TR3-overexpressing CWR22rv cells

FLAG-TR3 was excised from pcDNA3.FLAG-TR3 using *EcoR*V and *Hind*III, blunted, and inserted into pBI-EGFP at the *Nhe*I site to generate pBI-EGFP-FLAG-TR3. CWR22rv cells were transiently co-transfected with pUHDrtTA2S-M2 (TRE) (Dr. H. Bujard; ZMBH, Heidelberg, Germany) and pBI-EGFP-FLAG-TR3 or pBI-EGFP (EV; Clontech, Palo Alto, CA, USA) and then selected using 500 $ng.ml^{-1}$ G418 (Geneticin; Invitrogen, Carlsbad, California, US). The selected subclones were treated with 2 $\mu g.ml^{-1}$ doxycycline (Sigma, St. Louis, MO, USA). TR3 overexpression was confirmed by RT-PCR analysis.

Next-generation sequencing (NGS) high throughput RNA-Seq analysis

CWR22rv cells were infected with AdTR3 or AdCtrl, maintained for 24 h, and then harvested for RNA isolation followed by whole transcriptome analysis. RNA was converted to cDNA using a Clontech SMARTer Stranded RNA-Seq Kit with the proprietary SMART stranded N6 primer and SMARTScribeTM reverse transcriptase. The postcapture sequencing libraries were pooled and sequenced on the Illumina HiSeq 2500 platform using the 2 × 100 bp settings. Reads were mapped to the human genome reference HG19 using MapSplice. Gene expression was quantified using EdgeR and quantile normalized. Gene set enrichment analysis was performed using GSEA program and DAVID analysis on a preranked list of differentially expressed (> 1.5 fold) genes between AdTR3- and Ad-Ctrl-infected CWR22rv cells. Genes were clustered, and the difference in gene expression was classified using the MeV program. Novel splice variants were detected by aligning the novel splices against whole transcriptomes. Alterations in the splice junction rates between exons in full-length AR gene (AR8) were analyzed through Integrative Genomic Viewer (IGV) analysis.

Cross-linked RNA-immunoprecipitation (CLIP)

CWR22rv cells were infected with AdTR3 or AdCtrl, maintained for 24 h, and cross-linked with 1% formaldehyde (Sigma-Aldrich, St Louis, MO, USA) for 10 min. The fixed cells were then subjected to cross-linked RNA-immunoprecipitation (CLIP) analysis as previously described [12] with minor modifications. The protein-bound primary RNA fragments were enriched through immunoprecipitation with anti-hnRNP A2B1 antibodies (Supplementary Table S2). DNA contaminants were removed by treating with RNase-free

DNase (ThermoFisher Scientific, Rockford, IL, USA) at 37°C for 30 min, following which RNA fragments were obtained using chloroform extraction, and cDNA was synthesized using random hexamers (Enzynomics) and M-MLV Reverse transcriptase kit (Promega, Republic of Korea). Enrichment of AR pre-RNA fragments was analyzed via RT-PCR using the CLIP primers listed in Supplementary Table S1.

Single-strand RNA (ssRNA) protection assays

Thirty-mer ssRNA labeled with biotin at the 5' end (ssRNA oligo) was designed for RNA-protein interaction assays. ssRNA oligo sequence was identical to that found within Reg4, which contains one hnRNP A2B1 binding site overlapping with one HUB/HUR and two other HUB binding sites but has no hnRNP E1/E2 binding site. ssRNA oligo was incubated with or without the purified protein (FLAG-TR3 or splicing factors hnRNP A2B1 and HUB/HUR) in a binding buffer [20 mM Tris (pH 8.0), 0.5% sucrose, 1 mM DTT, 1 mM $MgCl_2$, 1 mM EDTA, and 2% glycerol in DEPC water] overnight at 4°C. RNA and protein degradation was minimized by adding RNase (RNasin) and protease inhibitors, respectively. Reactions were analyzed on a 3% horizontal agarose gel in TBE buffer containing 10 μg/ml EtBr. Gels were cooled and run in cooled TBE buffer. Free RNA and RNA-protein complex signals were detected using a UV transilluminator. ssRNA sequence is listed in Supplementary Table S1.

ssRNA oligo pull-down assays

The interactions between ssRNA oligo and proteins (hnRNP A2B1, hnRNP E1/E2, HUB/HUR, and TR3) were examined using ssRNA oligo pull-down assays as previously described [3], but with minor modifications. ssRNA oligo was immobilized onto AccuNanoBead™ Streptavidin Magnetic Nanobeads (400 nm, 5 mg/ml; Bioneer, Korea) for 1 h at 4°C in the presence of RNasin, brewel yeast tRNA (Roche, Basel, Switzerland), and salmon sperm-sheared DNA (ssDNA). Purified TR3 and splicing factor proteins were added into each interaction reaction in the presence of protease inhibitors and BSA. The interaction reactions were incubated overnight at 4°C. ssRNA oligo-bound proteins were analyzed using western blot analysis. RNA pull-down assay was also performed using whole cell lysates extracted from CWR22rv cells infected with AdTR3 or AdCtrl. Total proteins from each cell lysate were used in each binding reaction.

Xenograft animal model

Healthy and microbiologically monitored 4-week-old male NOD.CB17-Prkdc$^{SCID/J}$ mice, obtained from Korea Research Institute of Bioscience and Biotechnology (Daejeon, Korea), were gently injected with 100 µl of injectable anesthetics [Zoletil 50: Rompun: saline buffer (20:10:270)]. Mice were then warmed on a veterinary warming system. Inducible TR3-overexpressing (TR3; subline #2) or control (EV) CWR22rv cell clones (2×10^6 cells/site mixed 1:1 with Matrigel) were subcutaneously implanted into the shoulder of each mouse. The following day, mice were provided distilled water with or without 2 μg/ml doxycycline. Tumor size and volume were monitored and measured three times a week. Two days after the last tumor measurement, the animals were subjected to CO_2-induced euthanasia and sacrificed, and the tumors were extracted and weighed. Animals were maintained inside a cleaned bench in an animal room with a

12-h light/dark cycle and controlled temperature during all processes. The sterilized mouse cages, water, food, and bedding used for the animal study were replaced once a week. Ultra-fine II short needles (U-100 INSULIN 30 gauge 5/16” (8 mm) needle) were used for all injections to minimize any pain and lesions. Tumor volumes were calculated using the following formula: length × width × height × 0.5236 ($V = \pi \times L \times W \times H/6 = L \times W \times H \times 0.5236$) [13]. Statistical significance was calculated using two-tailed t-test analysis. p-value < 0.05 was considered statistically significant. All animal procedures were approved by the Institutional Animal Care and Use Committee (IACUC) of Chonnam National University (permit number: 2012-44). Animal experiments have been performed in accordance with the ARRIVE/NC3R guidelines.

Quantification and statistical analysis

Animal experiments were performed using six mice in each group. Data, which were obtained from more than three independent experiments, are presented as the mean ± SEM. Statistical significance was calculated using one-way ANOVA with Tukey’s post hoc test and two-tailed t-test analysis. p-value < 0.05 was considered statistically significant.

Results

TR3 regulates the expression of AR and AR-Vs in prostate cancer

To investigate the oncogenic function of TR3 in prostate cancer, we analyzed its expression profile in prostate tumors (Gene Expression Omnibus database) and evaluated the correlation between TR3 and AR expression levels in prostate tumor patients (The Cancer Genome Atlas database). We found that TR3 expression is upregulated in primary prostate tumors (Fig. 1A) and that its expression level is positively correlated with that of AR (Fig. 1B). Intriguingly, equally high levels of TR3 expression were observed in the loci adjacent to primary tumors. This is probably because immune deficiency and alteration of the tumor microenvironment by TR3 affects the physiology of tumor-adjacent cells, facilitating cancer progression [14]. In addition, TR3 expression was detected in all tested AR-positive prostate cancer cell lines, but not in AR-negative prostate cancer cell lines and was induced by 5α-dihydrotestosterone (DHT) (Fig. S1A), indicating TR3 as an androgen-responsive gene.

As TR3 and AR expression levels were positively correlated in prostate tumors, we investigated whether TR3 regulates AR expression. Overexpression of TR3 enhanced the protein levels of AR in androgen-independent CWR22rv cells and other AR-positive prostate cancer cells (LNCaP and C4-2) treated with or without androgen (Fig. 1C and Fig. S1B). Intriguingly, we observed other AR-Vs in TR3-overexpressing cells, which were absent in the controls (Fig. 1C). In addition, the mRNA levels of AR and AR-V7 were enhanced in these TR3-overexpressing cells treated with or without androgen, when examined using primers specifically covering exon 3/exon 4 (AR) and exon 3/CE3 (AR-V7) (Fig. 1D and Fig. S1C). Furthermore, TR3 overexpression increased the mRNA level of AR-V7 significantly more than that of the exon 1/exon 2-containing AR in CWR22rv cells (Fig. 1E), which was quantified through qPCR, pointing to the effects of TR3 on AR pre-mRNA splicing process as well as AR transcription. As expected, silencing

TR3 strongly decreased the protein and mRNA levels of AR and AR-Vs in AR-positive prostate cancer cells (Fig. 1F-G and Fig. S1D). In addition, treatment with the TR3 antagonist, DIM-C-pPhOH, strongly decreased the protein level of AR and AR-Vs in the presence or absence of DHT (Fig. S1E). However, in TR3-knockdown CWR22rv cells, the decreased AR and AR-V protein levels by TR3 silencing were not restored following treatment with MG-132 and chloroquine, which are blockers of protein degradation pathways (Fig. S1F), suggesting that TR3 regulates AR expression at mRNA level.

TR3 regulates the expression of AR splicing variants, altering splice junction rates between exons

The coupling of transcription and splicing processes is well-known [15–17]. Therefore, to further investigate the effects of TR3 on AR splicing process and expression, we first analyzed the potential binding sites of TR3 (TRE: AGGTCA) of TR3 ~ 5 kb upstream of the transcription start site and in the region covering the whole AR gene using Annhyb, a bioinformatics-based tool for sequence analysis. Four potential binding sites (P, A, B, and C) were found; site P was located ~ 3.4 kb upstream of the transcription start site, while the other three sites (A–C) were located within AR gene introns. Site A was located near the 3’ splicing site (3’ss) of exon 3, site B near the 5’ splicing site (5’ss) of CE3, and site C near the 5’ss of exon 4 (Fig. 2A). ChIP assays showed that TR3 might bind to all four sites; however, TR3 overexpression preferably enhanced TR3 binding to the regions containing sites P and C, but not sites A and B (Fig. 2B). These results suggest that TR3 binds to TREs in the AR gene and regulates its expression. However, we cannot rule out the possibility that TR3 binding to intron regions, especially to site C, affects AR pre-mRNA splicing process.

To investigate the alteration of AR splicing events in TR3-overexpressing prostate cancer cells, we performed next-generation sequencing (NGS) high-throughput RNA-Seq analysis of RNA obtained from TR3-overexpressing and control CWR22rv cells. The INDEL coupling with Integrative Genomic Viewer (IGV) analysis of RNA-Seq data of AR transcripts revealed that splice junction rates between exons within the pre-mRNA of full-length AR gene (AR8) were generally decreased (up to 50%) when TR3 was overexpressed in CWR22rv cells, while the splice junction rate between exon $1b_y$ and exon 2 increased (~ 30%) (Fig. 2C). The splicing between exon $1b_y$ and exon 2 has been identified in AR transcript variant 2 (also known as AR45), a short transcript that lacks exon 1, which is produced by utilizing an alternative transcription start site located between − 3 and + 5 of exon $1b_y$ [18]. Overexpression of AR45 may either repress or stimulate AR transactivation, depending on the cellular context.

We then validated the expression of AR splicing variants by performing RT-PCR analysis using specific primer pairs covering exon $1b_y$, exon 2, exon 3, cryptic exon CE1, cryptic exon CE3, and exon 4. The results showed that the increase in the level of RNA containing splice junctions between exon $1b_y$ and exon 2 (found in AR45) and exon 3 and CE3 (found in AR-V7) was higher than the general increase in total AR mRNA containing the exon 3–exon 4 junction, which was upregulated by TR3 activation of the AR promoter (Fig. 2D). Overexpression of TR3 also markedly increased the levels of RNA containing exon $1b_y$–exon 2 and exon 3–CE1 in C4-2 cells, whereas AR-Vs containing exon 3–CE1 or exon 3–CE3 were

hardly detectable in LNCaP cells (Fig. S2). These results suggest that TR3 affects the AR splicing process, especially in advanced CRPC cells, such as CWR22rv and C4-2 cells.

TR3 physically interacts with some splicing factors involved in AR splicing process

Because splicing factors and spliceosomal complexes play a crucial role in the regulation of the splicing process, we first examined whether TR3 overexpression altered the expression of some splicing factors, particularly NOVA-2, HUB (ELAV-like protein 2, ELAVL2), and other splicing factors involved in alternative splicing of AR pre-mRNA, such as hnRNP A2B1, hnRNP E1/E2, and HUR. RNA-Seq analysis revealed ~ 6.4-fold induction of NOVA-2 and ~ 1.7-fold induction of HUB in TR3-overexpressing cells compared with the control (Fig. 3A). The increase in NOVA-2 and HUB mRNA levels was confirmed through RT-PCR analysis (Fig. 3B), although western blot analysis results revealed that NOVA-2 protein level was only marginally increased (Fig. S3). Further, other splicing factors, such as hnRNP A2B1 and hnRNP E1/E2, were expressed at high basal levels in CWR22rv cells and showed no significant changes in their mRNA and protein levels upon TR3 overexpression.

hnRNP A2B1 plays a critical role in the control of the AR splicing process [7], and it likely interacts with TR3, based on the analysis of the protein interaction network [19]. Because the protein-protein interaction between TR3 and splicing factors might alter spliceosomal component recruitment and complex formation to control the AR splicing process, we investigated the physical interactions between TR3 and splicing factors (hnRNP A2B1, HUB/HUR, and hnRNP E1/E2) in TR3-overexpressing CWR22rv cells. Co-immunoprecipitation assays revealed that TR3 interacted with splicing factors hnRNP E1/E2 and hnRNP A2B1 (Fig. 3C). These results suggest that TR3 may be associated with spliceosomal complexes on AR pre-mRNA and may alter the splicing process.

TR3 overexpression alters the recruitment of some splicing factors near splicing sites, interacting with AR pre-mRNA

We further investigated whether TR3 altered the recruitment of splicing factors near splice sites. We chose 9 regions, designated Reg1–9, located ~ 1 kb upstream and/or downstream of the exon/intron junction of AR pre-mRNA and covering exons 1–4 (Fig. 4A). This is because spliceosomal components, such as snRNPs (U2/U2AF snRNP and U1 snRNP) and other hnRNPs, mostly bind to 3’ss and 5’ss of introns and branch sites [20], and the region covering exons 1–4 contains cryptic exons, which are frequently found in AR-Vs. Putative binding sites of some RBPs (hnRNP A2B1, hnRNP E1/E2, HUB/HUR, and NOVA2) in the 1.17-Mb AR pre-mRNA were investigated and found within Reg1–9, using SpliceAid program (a database of strictly experimentally assessed target RNA sequences in humans). Additionally, cross-linked RNA immunoprecipitation (CLIP) assays using anti-hnRNP A2B1 antibody and TR3-overexpressing or control CWR22rv cells revealed strong enrichment of hnRNP A2B1 at Reg4, which contains several putative hnRNP A2B1 binding sites, upon TR3 overexpression (Fig. 4B). We also detected the enrichment of hnRNP A2B1 at Reg9, which contains no putative binding site for hnRNP A2B1, but it has hnRNP E1/E2 and HUB/HUR binding sites. It is possible that hnRNP A2B1 enrichment at

Reg9 was due to protein-protein interactions between hnRNP A2B1 and other spliceosomal complex components.

To examine whether TR3 is associated with the spliceosomal complex at Reg4, we performed *in vitro* RNA-protein interaction assays involving single-strand RNA (ssRNA) protection and ssRNA oligo pull-down assays. A 30-mer ssRNA labeled with biotin at the 5' end (ssRNA oligo) was designed to include the sequence found within Reg4, which contains one hnRNP A2B1 binding site overlapping with one HUB/HUR and two other HUB binding sites, but it has no hnRNP E1/E2 binding site. ssRNA protection assays, which were performed using the ssRNA oligo and either purified TR3 or splicing factors (hnRNP A2B1 and HUB/HUR), showed that both TR3 and the splicing factors bound to and protected this ssRNA oligo from degradation (Fig. 4C). The ssRNA oligo migrated on agarose gel based on the formation of RNA-TR3 or RNA-splicing factor complex. Furthermore, ssRNA oligo pull-down assays performed using the same purified TR3 and splicing factors revealed that TR3 and the splicing factors, hnRNP A2B1 and HUB/HUR, bound to the ssRNA oligo (Fig. 4D). Together, these results suggest that TR3 binds to AR pre-mRNA and alters a recruitment of some splicing factors near splicing sites, which is a novel function of TR3.

TR3 enhances androgen-independent and androgen-dependent transactivation of ARs

We then examined the effect of TR3 on the transcriptional activity of ARs (full-length AR, AR-FL; AR N-terminal domain, AR-NTD; and AR-V7) based on luciferase reporter assays. The AR-NTD lacking LBD was used to represent the ligand-independent nature of AR, and AR-V7 was used to mimic AR-V behavior in CWR22rv cells. Overexpression of TR3 markedly enhanced both androgen-dependent and -independent transactivation of exogenous AR-FL, AR-NTD, and AR-V7 overexpressed in PPC1 cells in a dose-dependent manner (Fig. 5A–C and Fig. S4A–C). In addition, overexpression of TR3 significantly enhanced the androgen-induced transactivation of endogenous AR in androgen-dependent LNCaP cells (Fig. 5D). Blocking the function of TR3 using TR3-specific antagonist (DIM-C-pPhOH) impaired TR3-enhanced transactivation of AR-FL and AR-V7 (Fig. 5E-F). DIM-C-pPhOH not only inhibited the function of TR3 but also reduced TR3 protein level (Fig. S1E).

The subcellular localization of ARs and recruitment of coactivators to AR target genes are important for AR transactivation. TR3 overexpression promoted the nuclear translocation of ARs even in the absence of androgen (Fig. 5G). In addition, co-overexpression of TR3 seemed to facilitate the recruitment of AR coactivators, such as SRC-2, to the AR response element, synergistically enhancing the transactivation of AR (Fig. 5H). Furthermore, the physical interaction between TR3 and androgen-independent AR-NTD (Fig. S4D) suggests a molecular mechanism through which TR3 increases the activity of ARs in both an androgen-dependent and -independent manner. Collectively, these results show the profound effect of TR3 on the transactivation of ARs in prostate cancer, both in an androgen-dependent and -independent manner.

TR3 overexpression promotes prostate cancer cell proliferation and mobility, and enhances *in vivo* tumorigenesis of androgen-independent prostate cancer cells

RNA-Seq analysis showed the upregulation of genes that are involved in cell proliferation, migration, and invasion as well as the PI3K/AKT/MAPK signaling pathway when TR3 is overexpressed (Fig. 6A-B). PI3K/AKT/MAPK signaling is amplified as prostate cancer progresses into CRPC [21, 22]. Therefore, we further explored the function of TR3 in cell proliferation and mobility, which are the downstream cell behaviors of AR signaling. Overexpression of TR3 enhanced the proliferation of androgen-independent CWR22rv cells (Fig. 6C, left) as well as androgen-sensitive LNCaP cells under androgen-, outlaw IL6-, and forskolin-stimulated conditions (Fig. S5A). In contrast, TR3 silencing significantly inhibited the proliferation of these prostate cancer cells (CWR22rv and LNCaP) (Fig. 6C, right and Fig. S5B), which was confirmed using viability assays of TR3-knockdown CWR22rv cells (Fig. 6D). TR3 also affected cell mobility, with TR3 overexpression markedly increasing CWR22rv cell migration and invasion (Fig. 6E, left and 6F, top), and TR3 silencing resulting in a decrease in migration and invasion (Fig. 6E, right and 6F, bottom). These results suggest that TR3 increases cell proliferation and mobility of prostate cancer cells.

The effect of TR3 on prostate tumorigenesis was investigated using the inducible TR3-overexpressing (TR3) or control (EV) CWR22rv xenograft mouse models (Fig. S5C-D). We observed that the average volume of TR3 tumors was approximately 10-fold larger than that of EV tumors after ~ 7-week treatment with doxycycline (Fig. 6G-H). The average weight of tumors from TR3 mice was also approximately 10-fold greater than that of tumors from EV mice, although there were no significant differences in body weight (Fig. 6I-J). These results suggest the pivotal role of TR3 in *in vivo* tumorigenesis of advanced CRPC cells.

Discussion

Constitutive transcriptional activity of AR-Vs is important for prostate cancer progression. However, the molecular mechanisms underlying the production of AR-Vs remain unclear. In the present study, for the first time, we found a novel function of TR3, which controls AR splicing events in prostate cancer cells. Overexpression of TR3 upregulated the expression of mRNAs and proteins of smaller AR-Vs. Consistent with this finding, TR3 overexpression altered the splicing junction rates of AR pre-mRNA, resulting in the enhancement of mRNA levels of AR-Vs, such as AR45, AR-V7, and AR-V1, in advanced CRPC cells (CWR22rv and C4-2). We also demonstrated that TR3 overexpression alters the expression of certain splicing factors and that TR3 interacts with several known AR splicing factors (hnRNP A2B1 and hnRNP E1/E2) as well as the intron regions in AR pre-mRNA. Interestingly, TR3 functions in RNA splicing process while also regulating gene expression as a transcription factor. The association of TR3 with splicing factors and AR pre-mRNA might control the recruitment of spliceosomal complex components or identification of intron/exon boundaries.

Many splicing factors, including hnRNP A family (A0, A1/A1P10, and A2/B1) [7], hnRNP E1/E2 and HUR [6], proline-rich splicing factor PSF/SFPQ [23, 24], and U2AF1/U2AF65 [3], are involved in the splicing of AR-V7. Among them, PSF regulates AR splicing events by interacting with spliceosomal complex components as an integrator [23, 24]. It binds to the intronic region of AR transcripts and coordinates the complex formation of the spliceosome to promote the production of AR-V7 variant. Similar to PSF, TR3

directly or indirectly binds to the intronic region of AR transcripts at Reg4 and Reg9 and interacts with spliceosomal complex components, such as hnRNP A2B1 and hnRNP E1/E2. Many known RBPs contain the RNA recognition motif (RRM), KH, serine-rich, or poly-proline domains. Although the TR3 amino acid sequence does not contain RRM or KH domains, it has a putative poly-proline rich motif that shows high homology with that of PSF. These similarities suggest that TR3 may control AR splicing events as PSF does in prostate cancer cells.

The coupling of transcription and splicing processes is well-documented [15–17]. Transcription factors bound to the promoter or enhancers are likely involved in the recruitment of splicing factors to the site of transcription [15]. In addition, the C-terminal domain of RNA polymerase II (RNA pol II CTD) binds to some processing factors in the spliceosomal complexes and supports splicing factor recruitment to splice sites as shown with PSF and U2AF65-Prp19 complex [3, 23–25]. Interestingly, TR3 also interacts with RNA pol II CTD [19]. Therefore, TR3 overexpression may lead to the formation of alternative spliceosomal complexes by recruiting splicing factors to unusual splice sites through its interaction with RNA pol II CTD in AR pre-mRNAs, thus promoting the production of AR-Vs. In addition, TR3 bound to the intronic regions of the AR gene may directly recruit some splicing factors, such as hnRNP A2B1 and hnRNP E1/E2, through protein-protein interactions. Otherwise, it may indirectly change the local chromatin structure, thus inhibiting the splicing between exon 3 and exon 4 of AR-FL, which eventually promotes the production of small transcripts, such as AR-V7 [26].

TR3 overexpression causes immune deficiency and activates immune tolerance, which may create a potent immune suppressive tumor microenvironment during CRPC progression [27]. In the present study, RNA-Seq analysis revealed that TR3 overexpression significantly enhanced the expression of immune tolerance genes (Fig. S6A) while decreasing the expression of immune defense genes, particularly inflammatory genes (Fig. S6B-C), to allow tumor cell survival and escape from immune attack. Additionally, mature myeloid-derived suppressor cells (PMN-MDSCs) are important in CRPC progression, and the IL23-ROR-STAT3 axis signaling is activated when the proportions of circulating PMN-MDSCs are increased during CRPC progression [27]. Notably, the IL23-ROR-STAT3 signaling axis was upregulated when TR3 was overexpressed in CWR22rv cells (Fig. S6D-F). Collectively, these results suggest that TR3 promotes the susceptibility of prostate tumors to escape from immune checkpoints.

Conclusions

TR3 controls AR expression, splicing events, and androgen-independent function, and it likely alters immune responses to facilitate prostate tumorigenesis, suggesting that TR3 is a pivotal factor in prostate cancer progression. Therefore, TR3 could be an alternative therapeutic target for the treatment of advanced prostate cancer.

Abbreviations

AR: androgen receptor

ARE: androgen-response element

AR-Vs: androgen receptor variants

AR-FL: full-length AR

AR-NTD: AR N-terminal domain

CE3: cryptic exon 3

CLIP: cross-linked RNA-immunoprecipitation

CRPC: castration-resistant prostate cancer

DBD: DNA-binding domain

ELAVL1/2, ELAV-like protein 1/2

hnRNP: heterogeneous nuclear ribonucleoprotein

IGV: integrative Genomic Viewer

LDB: ligand-binding domain

NTD: NH2-terminal transactivation domain

pre-mRNA: precursor mRNA

PMN-MDSCs: mature myeloid-derived suppressor cells

RBPs: RNA-binding proteins

RNA pol II CTD: C-terminal domain of RNA polymerase II

RRM: RNA recognition motif

ssRNA oligo: thirty-mer ssRNA labeled with biotin at the 5’ end

TRE: TR3 response element or the potential binding sites of TR3

Declarations

Ethics approval and consent to participant

Four-week-old male NOD.CB17-PrkdcSCID/J mice were purchased from Korea Research institute of Bioscience and Biotechnology (KRIBB, Daejeon, Korea). All of the animal procedures were approved by the Institutional Animal Care and Use Committee (IACUC) of Chonnam National University (permit

number: 2012-44). Animal experiments have been performed in accordance with the ARRIVE/NC3R guidelines.

Consent for publication

Not applicable

Available data and materials

The datasets used and/or analyzed during the current study are available from the corresponding author on reasonable request.

Competing interests

The authors declare that they have no competing interests.

Funding

This research was supported by the Basic Science Research Program through the National Research Foundation of Korea (NRF) funded by the Ministry of Education, Science and Technology (NRF-2020R1A2C1006705).

Author's Contributions

K.L conceptualized the project. T.T.T designed and conducted the experiments and analyzed the data. T.T.T and K.L wrote the paper. Both authors discussed the results and reviewed the manuscript. K.L supervised the overall study.

Acknowledgments

We thank Dr. C. Jung for the kind gifts of C4-2 and CWR22rv cell lines. We are also grateful to Drs. J. J. Palvino and H. Bujard for providing pARE2-TATA-Luc and TetON system/pUHDrtTA2S-M2, respectively.

Authors' information

First author: Tuyen Thanh Tran, Ph.D., Postdoc, Laboratory of Developmental Genetics, School of Biological Sciences and Technology, Chonnam National University, Gwangju 61186, Republic of Korea. E-mail: thanhtuyentran2812@gmail.com

*Corresponding author: Keesook Lee, Ph.D., Professor, Laboratory of Developmental Genetics, School of Biological Sciences and Technology, Chonnam National University, Gwangju 61186, Republic of Korea. Phone: 82-62-530-0509, Fax: 82-62-530-0500. E-mail: klee@chonnam.ac.kr

References

1. Tan MH, Li J, Xu HE, Melcher K, Yong EL. Androgen receptor: structure, role in prostate cancer and drug discovery. Acta Pharmacol Sin. 2015;36:3–23.
2. Sprenger CC, Plymate SR. The link between androgen receptor splice variants and castration-resistant prostate cancer. Horm Cancer. 2014;5:207–17.
3. Liu LL, Xie N, Sun S, Plymate S, Mostaghel E, Dong X. Mechanisms of the androgen receptor splicing in prostate cancer cells. Oncogene. 2014;33:3140–50.
4. Li Y, Alsagabi M, Fan D, Bova GS, Tewfik AH, Dehm SM. Intragenic rearrangement and altered RNA splicing of the androgen receptor in a cell-based model of prostate cancer progression. Cancer research. 2011;71:2108–17.
5. Barbieri CE, Rubin MA. Genomic rearrangements in prostate cancer. Curr Opin Urol. 2015;25:71–6.
6. Yeap BB, Voon DC, Vivian JP, McCulloch RK, Thomson AM, Giles KM, Czyzyk-Krzeska MF, Furneaux H, Wilce MC, Wilce JA, Leedman PJ. Novel binding of HuR and poly(C)-binding protein to a conserved UC-rich motif within the 3'-untranslated region of the androgen receptor messenger RNA. J Biol Chem. 2002;277:27183–92.
7. Nadiminty N, Tummala R, Liu C, Lou W, Evans CP, Gao AC. NF-κB2/p52:c-Myc:hnRNPA1 Pathway Regulates Expression of Androgen Receptor Splice Variants and Enzalutamide Sensitivity in Prostate Cancer. Mol Cancer Ther. 2015;14:1884.
8. Gallo S, Arcidiacono MV, Tisato V, Piva R, Penolazzi L, Bosi C, Feo CV, Gafà R, Secchiero P. Upregulation of the alternative splicing factor NOVA2 in colorectal cancer vasculature. OncoTargets therapy. 2018;11:6049–56.
9. Safe S, Jin UH, Hedrick E, Reeder A, Lee SO. Minireview: role of orphan nuclear receptors in cancer and potential as drug targets. Mol Endocrinol. 2014;28:157–72.
10. Chang HUAC. Antisense TR3 Orphan Receptor Can Increase Prostate Cancer Cell Viability with Etoposide Treatment. Endocrinology. 1998;139:2329–34.
11. Lee SO, Abdelrahim M, Yoon K, Chintharlapalli S, Papineni S, Kim K, Wang H, Safe S. Inactivation of the orphan nuclear receptor TR3/Nur77 inhibits pancreatic cancer cell and tumor growth. Cancer Res. 2010;70:6824–36.
12. Gagliardi M, Matarazzo MR. RIP: RNA Immunoprecipitation. Methods Mol Biol. 2016;1480:73–86.
13. Heitjan DF, Manni A and Santen RJ. Statistical Analysis of < em > in Vivo Tumor Growth Experiments. Cancer Research 1993; 53: 6042–6050.
14. Hanna RN, Carlin LM, Hubbeling HG, Nackiewicz D, Green AM, Punt JA, Geissmann F, Hedrick CC. The transcription factor NR4A1 (Nur77) controls bone marrow differentiation and the survival of Ly6C- monocytes. Nat Immunol. 2011;12:778–85.
15. Nogués G, Kadener S, Cramer P, de la Mata M, Fededa JP, Blaustein M, Srebrow A, Kornblihtt AR. Control of alternative pre-mRNA splicing by RNA Pol II elongation: faster is not always better. IUBMB Life. 2003;55:235–41.

16. McCracken S, Fong N, Yankulov K, Ballantyne S, Pan G, Greenblatt J, Patterson SD, Wickens M, Bentley DL. The C-terminal domain of RNA polymerase II couples mRNA processing to transcription. Nature. 1997;385:357–61.
17. David CJ, Boyne AR, Millhouse SR, Manley JL. The RNA polymerase II C-terminal domain promotes splicing activation through recruitment of a U2AF65-Prp19 complex. Genes Dev. 2011;25:972–83.
18. Ahrens-Fath I, Politz O, Geserick C, Haendler B. Androgen receptor function is modulated by the tissue-specific AR45 variant. The FEBS Journal. 2005;272:74–84.
19. Vinayagam A, Stelzl U, Foulle R, Plassmann S, Zenkner M, Timm J, Assmus HE, Andrade-Navarro MA, Wanker EE. A directed protein interaction network for investigating intracellular signal transduction. Sci Signal. 2011;4:rs8.
20. Craig NL. Molecular Biology: Principles of Genome Function. Oxford University Press; 2010.
21. Pienta KJ, Bradley D. Mechanisms underlying the development of androgen-independent prostate cancer. Clin Cancer Res. 2006;12:1665–71.
22. Feldman BJ, Feldman D. The development of androgen-independent prostate cancer. Nat Rev Cancer. 2001;1:34–45.
23. Takayama K-i, Suzuki T, Fujimura T, Yamada Y, Takahashi S, Homma Y, Suzuki Y, Inoue S. Dysregulation of spliceosome gene expression in advanced prostate cancer by RNA-binding protein PSF. Proceedings of the National Academy of Sciences 2017; 114: 10461–10466.
24. Dong X, Sweet J, Challis JR, Brown T, Lye SJ. Transcriptional activity of androgen receptor is modulated by two RNA splicing factors, PSF and p54nrb. Mol Cell Biol. 2007;27:4863–75.
25. Emili A, Shales M, McCracken S, Xie W, Tucker PW, Kobayashi R, Blencowe BJ, Ingles CJ. Splicing and transcription-associated proteins PSF and p54nrb/NonO bind to the RNA polymerase II CTD. RNA. 2002;8:1102–11.
26. Rambout X, Dequiedt F, Maquat LE. Beyond Transcription: Roles of Transcription Factors in Pre-mRNA Splicing. Chem Rev. 2018;118:4339–64.
27. Arianna calcinotto CS, Zagato E, Mitri DD, Gil V, Mateus crespo, Gaston De Bernardis, Marco losa, Michela Mirenda, Emiliano Pasquini, et al. IL-23 secreted by myeloid cells drives castration-resistant prostate cancer. Nature 2018; 559: 363–389.

Figures

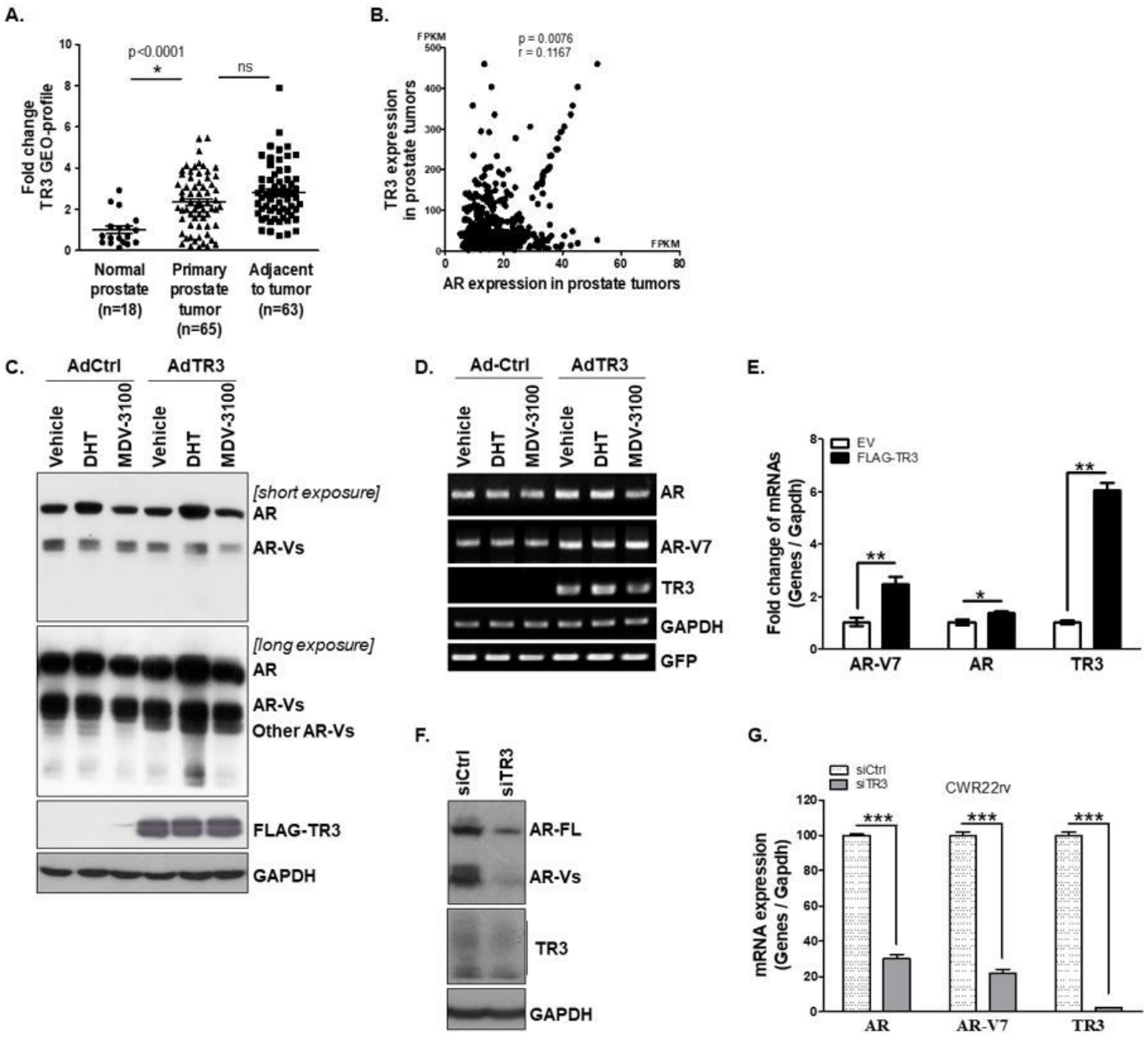

Figure 1

TR3 regulates the expression of AR and AR-Vs in prostate cancer. A, Elevation of TR3 in prostate tumors. The graph shows TR3 mRNA levels in normal human prostate (n=18), primary prostate tumor (n=65), and the region adjacent to the prostate tumor (n=63). The data were extracted from the public RNA-Seq database established by the Pathology Department of Houston Methodist University Hospital. Data are shown as mean ± SEM. *, p<0.001; ns, not significant; one-way ANOVA analysis with Tukey's post hoc test. B, Positive correlation between TR3 and AR levels in prostate tumors. Scatter plot showing a positive correlation between TR3 and AR expression in TCGA Prostate Tumors' Pathology Atlas Database (n=498). The x and y axes denote fragments per kilobase of transcript per million mapped reads (FPKM). Pearson p and r values were analyzed using correlation analysis with two-tailed Spearman test. C-E, TR3 overexpression increases the expression levels of AR and AR-Vs. Western blot (C) and RT-PCR (D) analysis showed the protein levels of AR and AR-Vs, and the appearance of other AR-Vs in AdTR3- or

AdCtrl-infected CWR22rv cells, which were treated with 10 nM DHT, 10 μM MDV-3100 or vehicle only. GFP was used as a control for the efficiency of adenovirus infection. qPCR analysis showed alterations in the level of AR mRNAs, which contain exon 1–exon 2 (AR) and exon 3–CE3 (AR-V7) in CWR22rv cells transfected with FLAG-TR3 or empty vector (EV) (E). F-G, Silencing of TR3 expression or inhibiting of TR3 function significantly decreases the expression levels of AR and AR-Vs. Western blot analysis showing AR and AR-V protein levels in CWR22rv cells silenced with siTR3 (F). qPCR analysis showing AR, AR-Vs and TR3 mRNA levels in CWR22rv cells transfected with siTR3 or siCtrl (G). Data are shown as mean ± SEM. *, p<0.05; **, p<0.01; ***, p<0.001; one-way ANOVA analysis with Tukey's post hoc test.

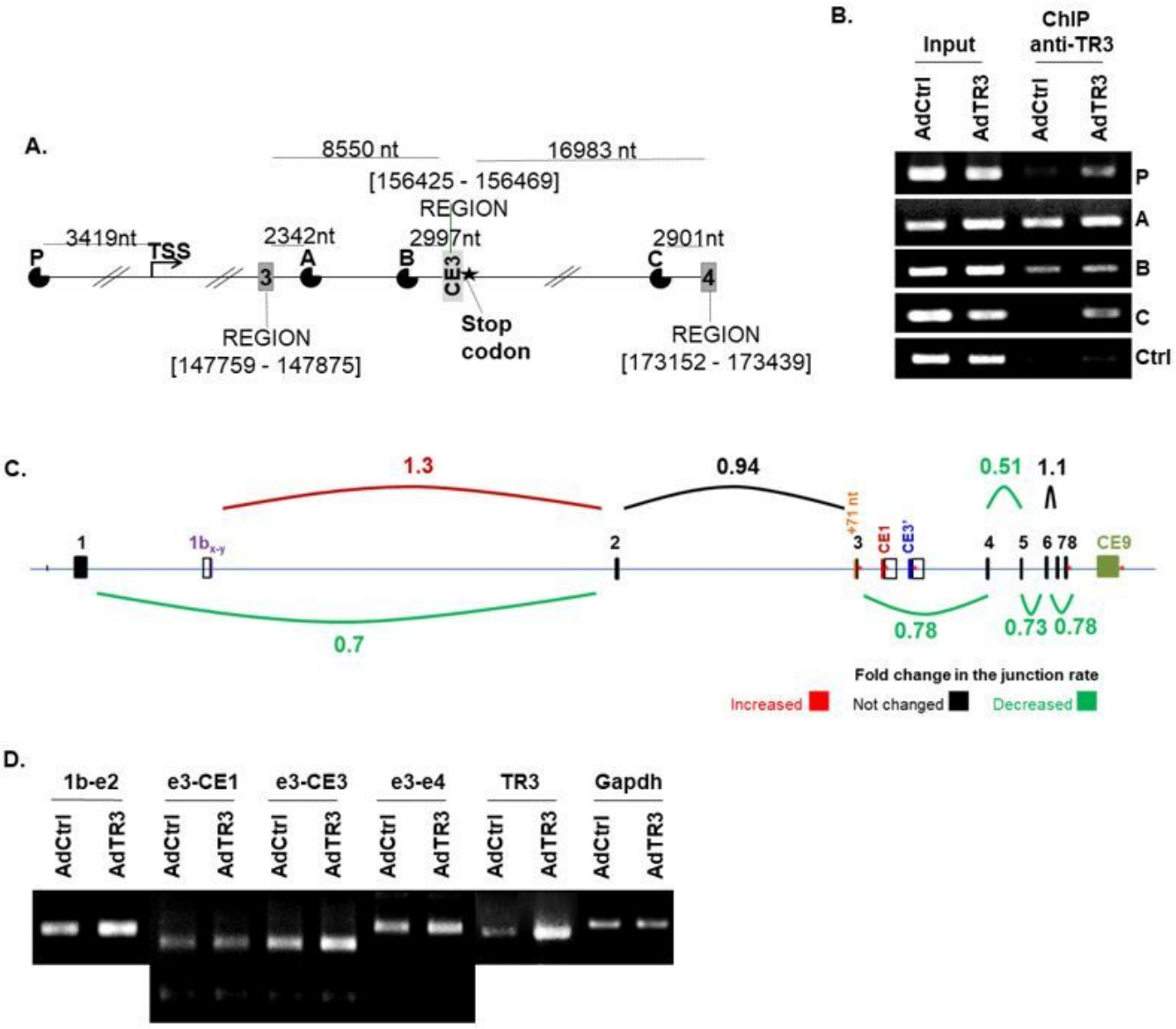

Figure 2

TR3 regulates the expression of AR splicing variants, altering splice junction rates between exons. A–B, TR3 binds to the promoter and intron regions of AR gene. Schematic presentation of putative TR3 binding sites (P, A, B, and C) in AR gene (A). Recruitment of TR3 protein to putative TR3 binding sites within the

promoter and intron regions of AR gene was determined via ChIP assays using anti-TR3 antibody (B). CWR22rv cells were infected with AdTR3 or AdCtrl. Changes in TR3 enrichment at putative TR3 binding sites was examined using PCR. The loading control (Ctrl) was β-actin. C-D, TR3 overexpression alters the splice junction rate between exons of AR pre-mRNA. CWR22rv cells were infected with AdTR3 or AdCtrl, and the samples were analyzed using Next-Generation Sequencing (NGS) high-throughput RNA-Seq analysis. Splice junction rate between exons within the pre-mRNA of AR-FL (AR8) was analyzed using Integrative Genomic Viewer (IGV) analysis (C). RT-PCR analysis showed alterations of the splice junction rate between AR-V exons, particularly exon 1by/exon 2 and exon 3/CE3 (D).

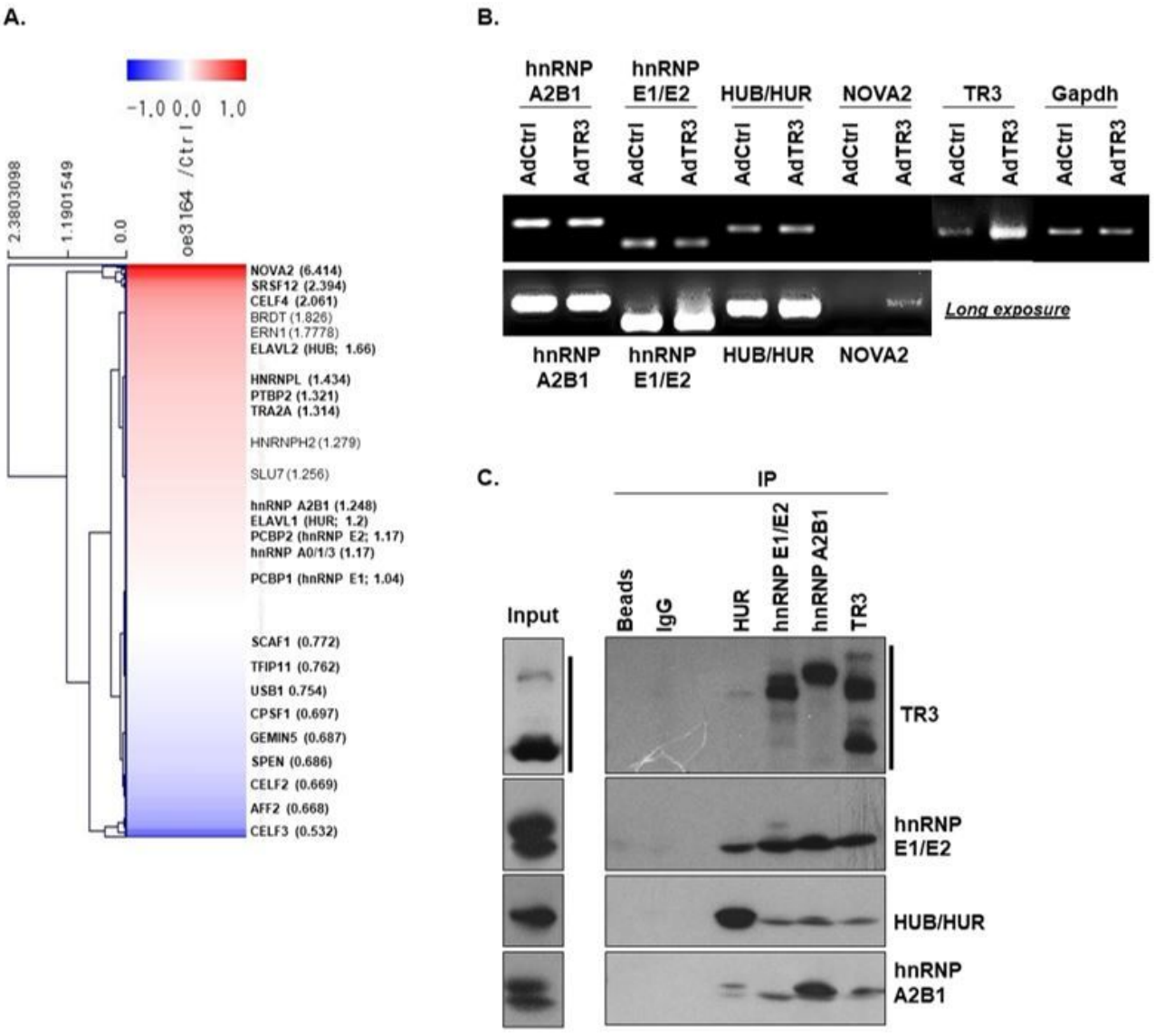

Figure 3

TR3 physically interacts with some splicing factors involved in AR splicing process. A-B, TR3 overexpression alters the expression level of some factors involved in the splicing of AR pre-mRNA. Heatmap of RNA-seq data showing alterations in the expression level of some splicing factors in TR3-

overexpressing CWR22rv cells (A). RT-PCR analysis presenting mRNA levels of several splicing factors (hnRNP A2B1, hnRNP E1/E2, HUB/HUR, and NOVA-2) in CWR22rv cells infected with AdTR3 or AdCtrl (B). C, TR3 physically interacts with splicing factors involved in the splicing of AR pre-mRNA. Immunoprecipitation (IP) analysis showed physical interactions between TR3 and several splicing factors (hnRNP A2B1, hnRNP E1/E2, and HUB/HUR) in CWR22rv cells infected with AdTR3. Immunoprecipitation was performed using anti-TR3, anti-hnRNP A2B1, anti-hnRNP E1/E2, and anti-HUR antibodies. Protein levels were analyzed via western blot analysis using anti-TR3, anti-hnRNP A2B1, anti-hnRNP E1/E2, and anti-HUR antibodies.

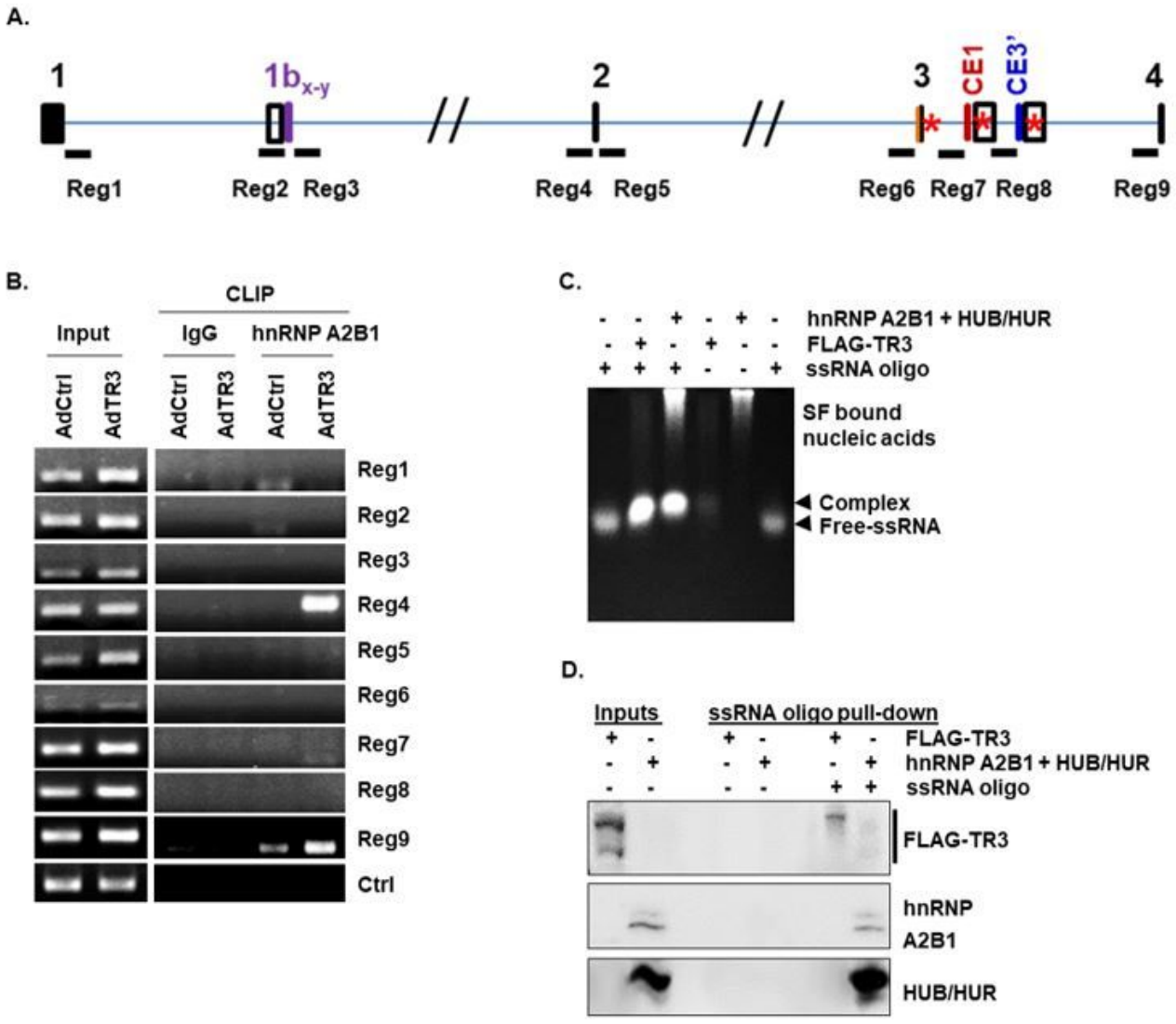

Figure 4

TR3 overexpression alters the recruitment of some splicing factors near splicing sites, interacting with AR pre-mRNA. A-B, TR3 overexpression alters the recruitment of some splicing factors to AR pre-mRNA. Schematic presentation of intronic regions marked Reg1–9 in AR pre-mRNA, which were selected for CLIP

analysis (A). CLIP analysis using anti-hnRNP A2B1 antibody showed an enrichment of hnRNP A2B1 at Reg4 and Reg9 within AR pre-mRNA in TR3-overexpressing CWR22rv cells (B). C-D, TR3 interacts with AR pre-mRNA. ssRNA protection assays performed using purified TR3 and splicing factors (hnRNP A2B1 and HUB/HUR) showed protection of a 30mer ssRNA oligo of AR-Reg4 labelled with biotin at the 5' end (ssRNA oligo) (C). ssRNA pull-down assays performed using the same purified protein fractions show the binding of TR3 and splicing factors to ssRNA oligo (D). Protein levels were analyzed via western blot analysis using anti-TR3, anti-hnRNP A2B1, and anti-HUR antibodies.

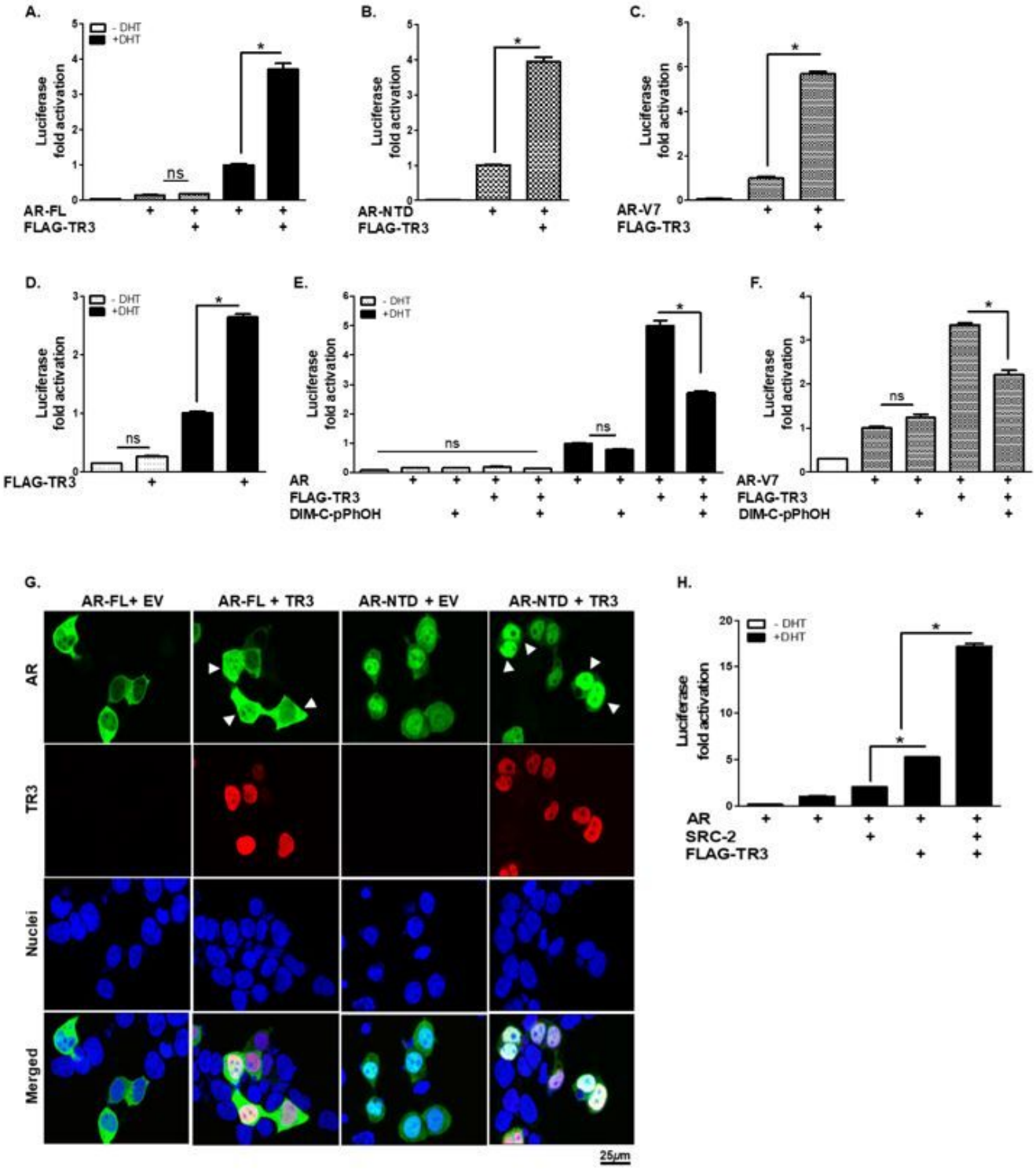

Figure 5

TR3 positively regulates the transactivation of ARs in both androgen-dependent and androgen–independent manners. TR3 enhances the androgen-dependent and -independent transactivation of ARs. A-D, TR3 overexpression significantly enhances the transactivation of ARs. Both PPC1 cells overexpressed with AR-FL (A), AR-NTD (B), or AR-V7 (C), and LNCaP cells (D) were transiently transfected with FLAG-TR3 or empty vector (EV) along with pARE2-TATA-luc and treated with 1 nM DHT or vehicle. E-F, TR3-mediated enhancement of the transactivation of ARs was impaired by treatment with TR3 antagonist (DIM-C-pPhOH). PPC1 cells were co-transfected with AR-FL (E) or AR-V7 (F) together with FLAG-TR3 or EV along with pARE2-TATA-luc and treated with 20 μM or vehicle in the presence or absence of 10 nM DHT. G, TR3 increases androgen-independent nuclear translocation of ARs. HEK 293T cells were transfected with GFP-AR-FL or GFP-AR-NTD together with TR3 or EV in the absence of androgen. Subcellular localizations of ARs and TR3 were detected as green fluorescent protein (GFP) and red Alexa Fluor568 signal, respectively. Nuclei were stained blue with TOPRO-3. Arrowheads indicate strong signals of nuclear-localized AR proteins in TR3-coexpressing cells. Images were acquired using a confocal microscope. Scale bars, 25 μm. H. TR3 overexpression enhances coactivator recruitment to AR. PPC1 cells were co-transfected with AR, SRC-2, and FLAG-TR3 or empty vector along with pARE2-TATA-luc and incubated with or without 1 nM DHT. Data are shown as mean ± SEM. *, $p<0.001$; ns, not significant; one-way ANOVA with Tukey's post hoc test.

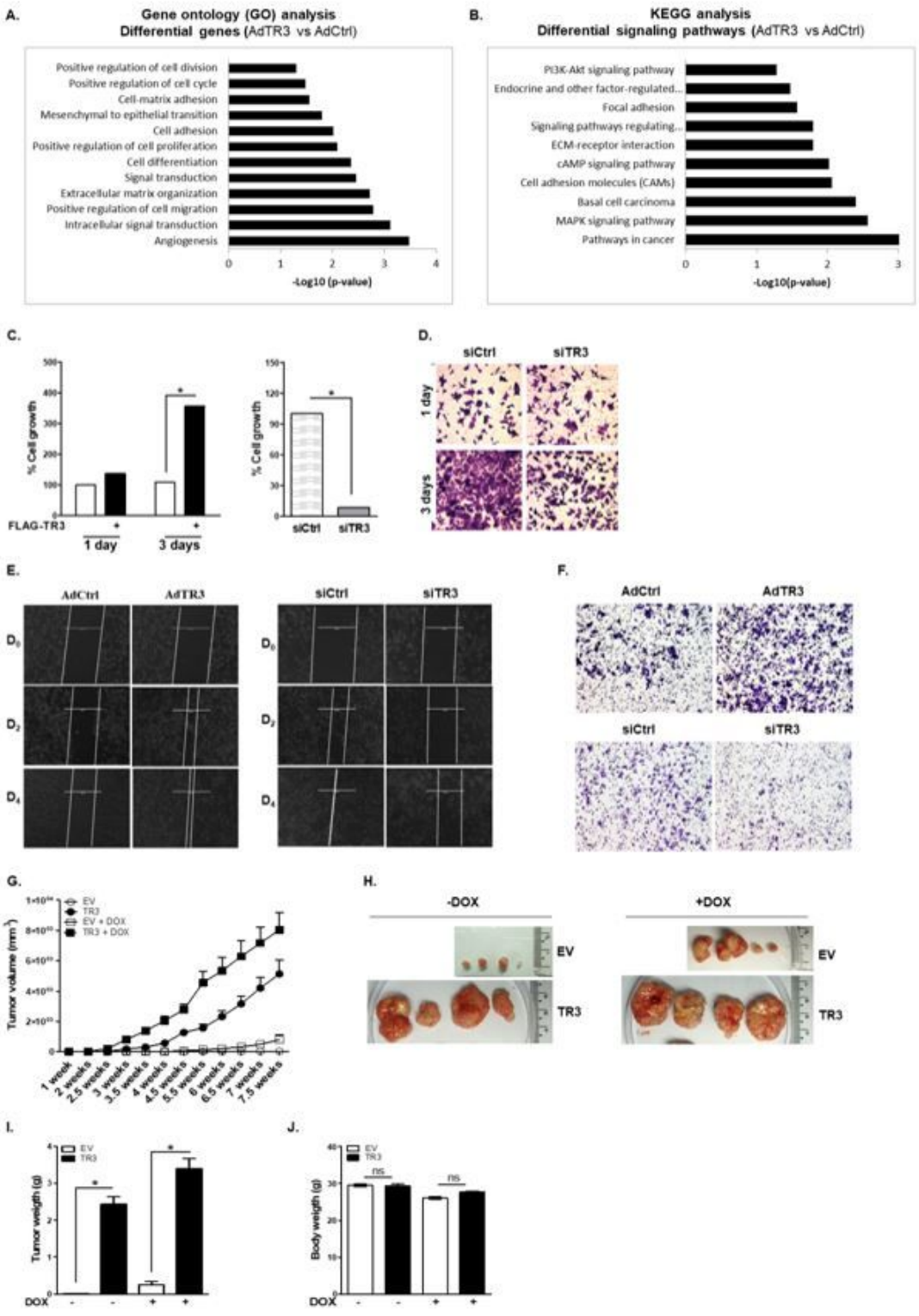

Figure 6

TR3 overexpression enhances cell proliferation and mobility, and in vivo tumorigenesis of androgen-independent prostate cancer cells. A-B, TR3 overexpression enhances cellular signaling crucial for prostate cancer progression. RNA-Seq analysis was performed on CWR22rv cells infected with AdTR3 or AdCtrl. The gene oncology (GO) (A) and KEGG (B) analysis of RNA-Seq data show upregulated expression of genes and enhanced signaling pathways. C, TR3 regulates androgen-independent prostate cancer cell

proliferation. Percent cell growth of TR3-overexpressing (C, left) or TR3-knockdown (C, right) CWR22rv cells. Data are shown as mean ± SEM. *, p<0.001; two-tailed t-test. D, TR3 knockdown significantly reduced the viability of CWR22rv cells. Cells were silenced using siTR3 or siCtrl for 1 day and 3 days, stained with Crystal Violet, and imaged using ZEISS microscopy at 20X magnification. E-F, TR3 regulates androgen-independent prostate cancer cell mobility. Scratch-wound healing assay of CWR22rv cells infected with AdTR3 or AdCtrl (E, left) and cells transfected with siTR3 or siCtrl (E, right). Scratch-wounds were generated and the wound distances were monitored for 2 (D2) and 4 (D4) days. Invasion assays of CWR22rv cells infected with AdTR3 or AdCtrl (F, top) and cells transfected with siTR3 or siCtrl (F, bottom). Cell invasion was allowed to occur for 48 h, stained with crystal violet, and imaged using ZEISS microscopy at 20X magnification. G-J, TR3 overexpression robustly promotes androgen-independent CWR22rv xenograft tumor growth in vivo. The inducible TR3-overexpressing (TR3; subline #2) or control (EV) CWR22rv cell clones were implanted into shoulders of 4-week-old male NOD.CB17-PrkdcSCID/J mice, and the mice were supplied with distilled water containing or not containing 2 μg/ml doxycycline (DOX) for 7 weeks. Tumor size and volume were measured three times per week for 7 weeks. Tumor volumes (G) measured for 7 weeks, and representative tumors (H) dissected from mice after 7 weeks. Tumor weight (I) and body weight (J) measured after 7 weeks. Data are shown as mean ± SEM, n=2 independent biological in vivo experiments (n=6 mice per each group). *, p<0.001; ns, not significant; two-tailed t-test.

Supplementary Files

This is a list of supplementary files associated with this preprint. Click to download.

- TR3Supplementary.docx